LANGMUIR

pubs.acs.org/Langmuir Article

Janus Liposomes: Exploring Liquid−Liquid Phase-Separating Lipid Systems Alternative to DOPC/DPPC/Cholesterol

Ayesha Akter and Wei Zhan*

Cite This: *Langmuir* 2025, 41, 19270−19281 Read Online

ACCESS | Metrics & More | Article Recommendations | Supporting Information

ABSTRACT: Existing work on Janus liposomes almost exclusively employs the ternary lipid system based on 1,2-dioleoyl-*sn*-glycero-3-phosphocholine (DOPC), 1,2-dipalmitoyl-*sn*-glycero-3-phosphocholine (DPPC), and cholesterol (Chol), offering limited material choice, stability, and operating temperature window. In this work, we have systematically investigated >30 binary/ternary lipid combinations as potential alternatives to DOPC/DPPC/Chol to produce microsized Janus liposomes. A variety of structural/chemical differentiators are explored to induce phase separation in these systems, such as chain length (C10 to C18), unsaturation level (1 to 3 double bonds per acyl chain) and headgroup identity (phosphatidylcholine, phosphatidylglycerol and sphingomyelin). Using confocal fluorescence microscopy, we have identified eight new Chol-containing systems that produce Janus liposomes in decent to high yields. Furthermore, we also discover that global liquid−liquid phase separation can occur within individual Chol-free, binary liposomes, despite at much lower yields compared to Chol-containing systems. Evaluating these successful cases together with other tested systems, we also attempt to provide a set of guidelines for designing and preparing phase-separated liposomes. These findings may be of value to workers in membrane biophysics, particularly related to lipid liquid−liquid phase separation, as well as those interested in exploring Janus liposomes as an anisotropic colloidal material, for example, in liposomal drug delivery and active matter.

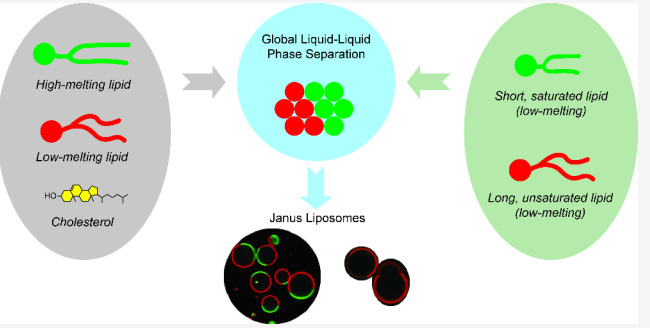

INTRODUCTION

The dynamic ongoing research on Janus/patchy particles[1−4] has prompted a number of recent investigations into lipid-assembled colloidal particles with broken symmetry, i.e., Janus liposomes (JLs).[5−10] Compared to their inorganic/polymer-based counterparts, which are typically hard-set, Janus liposomes are unique in that their molecularly assembled architecture is not only intrinsically biocompatible but also highly amenable to payload incorporation and encapsulation—features underpinning the broad use of liposomes in drug delivery,[11−13] food processing[14] and cosmetics.[15] With respect to conventional (homogeneous) liposomes, furthermore, the broken symmetry carried by Janus liposomes adds an entirely new dimension for design and function enhancement of these colloidal particles, e.g., in hierarchical superassemblies,[16,17] nano/micromotors[18,19] and active matter.[20,21] Currently, however, there exists only a very limited material inventory from which such anisotropic liposomes can be made—an issue this work seeks to address.

Existing work on Janus liposomes[5−10] almost exclusively employs the ternary lipid system based on 1,2-dioleoyl-*sn*-glycero-3-phosphocholine (DOPC), 1,2-dipalmitoyl-*sn*-glycero-3-phosphocholine (DPPC) and cholesterol (Chol), which can phase separate into two immiscible liquid domains in liposomes at certain mixing ratios at room temperature.[22−24] While DPPC and Chol are accumulated in the liquid-ordered (l_o) domain, DOPC makes up the majority of the liquid-disordered (l_d) domain.[25,26] Besides lipid distribution, the two domains also differ significantly from each other in their thickness,[27,28] mechanical properties,[29,30] lipid diffusion/fluidity,[31,32] and hydration level.[33,34] Critical to such liquid/liquid immiscibility is Chol's unique ability to maintain differential interactions with the other two components. In the l domain, it loosens up tight chain condensation of DPPC by occupying the pocket between palmitoyl chains,[35,36] effectively liquefying the latter—without Chol, DPPC would assemble into a condensed gel phase at room temperature; in the l_d domain, on the other hand, Chol enhances the chain ordering of DOPC by limiting the latter's rotation around its double bond.[36−38] The fact that liquid−liquid phase separation has yet to be realized in sterol-free, nonsurface-bound lipid systems[39] further testifies Chol's unique multivalence in this regard.

Received: April 6, 2025
Revised: July 5, 2025
Accepted: July 7, 2025
Published: July 14, 2025

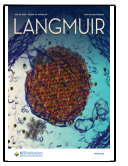

https://doi.org/10.1021/acs.langmuir.5c01698
Langmuir 2025, 41, 19270−19281

While the DOPC/DPPC/Chol system has been absolutely essential in demonstrating the feasibility of making Janus liposomes and revealing some key features of this class of anisotropic particles, potential benefits of having alternative systems are evident and many. These include 1) Systems featuring a more broadly accessible liquid/liquid coexistence region, which would enable greater composition control of liposome products; 2) Systems operating with a wider temperature window. In this regard, phase separation in DOPC/DPPC/Chol is limited by the melting temperature of DPPC (41 °C), toward which the two liquid domains tend to coalesce,[22,40] thus losing its Janus configuration; and 3) Systems with better chemical stability. Here, for example, lipids with unsaturated acyl chains such as DOPC are prone to oxidation.[41,42] Functionality aside, variety is also needed to enable a robust and holistic approach to Janus liposomes research.

Lipid segregation tends to occur when the repulsive interactions between dissimilar lipids surpass their adhesive association. In lipid bilayers, the prevalent form of lipid organization, such separation proceeds laterally in a largely 2D lipid environment, with their aligned polar groups shielding hydrophobic acyl chains from water on both sides. Within this dynamic formation, repulsion between lipids can come about in several flavors. These include: 1) Mismatched acyl chains, which can take effect via chain length (e.g., DLPC/DPPC),[43,44] (un)saturation level (e.g., DOPC/DPPC)[23] or bulkiness/branching (e.g., DPhPC/DPPC);[45] 2) Incompatible headgroups, which may arise due to differences in their physical size or hydrogen-bonding ability (e.g., DPPE vs DPPG);[46,47] and 3) Favorable combinations of dissimilar headgroups and chains. For example, while DOPC and DOPE mix homogeneously in the presence of Chol, switching DOPE to DPPE induces phase separation.[48] Besides these intrinsic dissimilarities, phase separation can also be facilitated by extraneous agents that bind/complex specific components in lipid mixtures, of which Ca^{2+}-triggered segregation of anionic lipids serves a well-known example.[49,50] Depending on the type/composition of lipids and temperature, phase separation eventually evolves into a certain combination of gel, l_d and l_o phases.

It is important to also note that lipid phase separation does not spontaneously lead to Janus liposomes. From topology's standpoint, only in the case of liquid/liquid phase separation (LLPS) can lipids be mobile enough to continuously coalesce, eventually ripening into two hemispherical domains separated by a single global phase boundary (Figure 1). By contrast, phase separation involving gel phase typically yields uncircular or jagged boundary lines due to its frozen coalescence processes characteristic of retarded lipid diffusion/exchange.[51] Even within the regime of LLPS, moreover, the desired Janus configuration may still elude individual liposomes if kinetically trapped small domains are relatively long-lived with respect to the two-faced arrangement.[23,52] In this case, LLPS in the system will remain local and nanoscopic (Figure 1), unable to reach two-faced Janus configuration on a practical time scale. In this regard, therefore, LLPS should be taken only as a necessary, but not sufficient, condition for producing Janus liposomes.

In this work, we have systematically investigated >30 binary/ternary lipid combinations as potential alternatives to DOPC/DPPC/Chol to produce microsized Janus liposomes. A variety of structural/chemical differentiators are explored to induce phase separation in these systems, such as chain length (C10 to C18), unsaturation level (1 to 3 double bonds per acyl chain) and headgroup identity (phosphatidylcholine, PC, phosphatidylglycerol, PG, and sphingomyelin, SM). Using confocal fluorescence microscopy, we have identified eight new systems that produce Janus liposomes in decent to high yields. Comparing these successful cases with other tested systems, we also attempt to formulate a set of guidelines for designing and preparing phase-separated lipid systems. Furthermore, we also discover that global LLPS can occur within individual sterol-free binary liposomes, despite at much lower yield compared to those with Chol. These findings may be of value to workers in membrane biophysics, particularly related to lipid liquid−liquid phase separation, and to those interested in exploring Janus liposomes as a new functional material, e.g., in liposomal drug delivery and active matter.

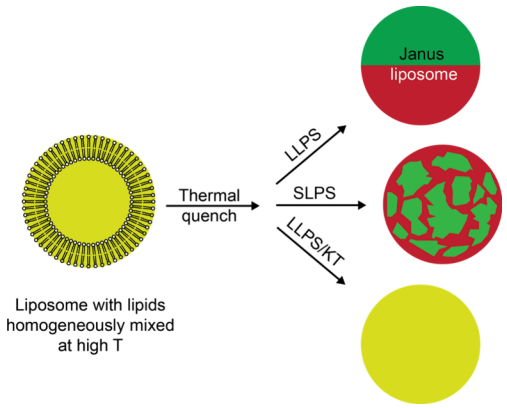

Figure 1. Different topological outcomes of phase separation in liposomes featuring lipid liquid/liquid phase separation (LLPS), solid/liquid phase separation (SLPS), and liquid/liquid phase separation with kinetically trapped local states (LLPS/KT). Lipid domains are depicted by different colors for completely separated phases (green and red) and homogeneous (or nanoscopically mixed) phases (yellow).

EXPERIMENTAL SECTION

Reagents and Materials. Lipids, including 1,2-dipalmitoyl-*sn*-glycero-3-phosphocholine (DPPC), *N*-palmitoyl sphingomyelin (d18:1/16:0) (PSM), 1,2-dilauroyl-*sn*-glycero-3-phosphocholin (12:0 PC, or DLPC), 1,2-ditridecanoyl-*sn*-glycero-3-phosphocholine (13:0 PC), 1,2-dimyristoyl-*sn*-glycero-3-phosphocholine (14:0 PC, or DMPC), 1,2-dilauroyl-*sn*-glycero-3-phospho-(1′-*rac*-glycerol) (sodium salt) (12:0 PG, or DLPG), 1,2-dioleoyl-*sn*-glycero-3-phosphocholine (18:1 PC, or DOPC), 1,2-diphytanoyl-*sn*-glycero-3-phosphocholine (4ME 16:0 PC, or DPhPC), 1,2-dipalmitoleoyl-*sn*-glycero-3-phosphocholine (16:1 PC), 1,2-dilinoleoyl-*sn*-glycero-3-phosphocholine (18:2 PC), 1,2-dilinolenoyl-*sn*-glycero-3-phosphocholine (18:3 PC), 1,2-dioleoyl-*sn*-glycero-3-phospho-(1′-*rac*-glycerol) (sodium salt) (18:1 PG, or DOPG), 1,2-didecanoyl-*sn*-glycero-3-phospho-*L*-serine (sodium salt, DDPS), 1,2-dioleoyl-*sn*-glycero-3-phosphoethanolamine-*N*-(lissamine rhodamine B sulfonyl) (ammonium salt) (rho-DOPE), and 23-(dipyrrometheneboron difluoride)-24-norcholesterol (Bodipy-Chol), were obtained from Avanti Polar Lipids (Alabaster, AL). All lipids were received as solutions dissolved in chloroform except PSM and DLPG; the latter were received in powder form and dissolved in 4:1 (v:v) chloroform and methanol before use. Other chemicals, including poly(vinyl alcohol) (PVA, MW: 145,000), cholesterol, chloroform, and methanol, were purchased from Sigma-Aldrich. Deionized water was produced from a Mili-Q water system (IQ 700, Millipore) with resistivity >18.2 MΩ-cm and TOC level <2.1 ppb.

https://doi.org/10.1021/acs.langmuir.5c01698
Langmuir 2025, 41, 19270−19281

Liposome Preparation. Microsized Janus liposomes were prepared with the gel-assisted lipid hydration method as previously described.[8−10] To start, lipid precursors in chloroform were first prepared by mixing certain amounts of low-/high-melting lipids, cholesterol and small quantities of lipid phase-indicating dyes. In all cases, low levels of rhodamine-labeled DOPE (rho-DOPE, l_d) and (/or) Bodipy-labeled cholesterol (Bodipy-Chol, l_o) were also included in the lipid precursors as phase indicators. The total lipid concentration of these precursors was typically ∼5 mM and their specific mole mixing ratios are given in the main text as they appear. Separately, PVA gel films on glass slides were prepared by spreading drops of an aqueous PVA solution (5 wt %) over precleaned glass slides (VWR Vistavision microscope slide, dimensions: 75 × 25 × 1 mm), followed by drying on a hot plate at 50 °C for 30 min. On such dried PVA films, thin lipid stacks were then deposited by spreading ∼5 μL of lipid precursors over the entire surface of the PVA-coated glass slides. The resultant gel-supported lipids were subsequently dried under vacuum for 1h at room temperature. To produce liposomes, finally, thus-formed lipid stacks were hydrated in 1 mL DI water in a sealed chamber for 1h at either 50 or 60 °C as specified in the main text. The final liposome products are stored at 4 °C in the dark before further use.

Confocal Fluorescence Microscopy. Fluorescence imaging was performed on a Nikon A1+/MP confocal scanning laser microscope (Nikon Instruments, Inc. Melville, NY) with 10× and 20× objective and excitation laser lines at 488 and 561 nm. The corresponding green and red emission signals were filtered at 525 ± 25 and 595 ± 25 nm, respectively.

Liposome samples used for imaging typically contain 5 μL liposome solutions held in PDMS reservoirs fixed on preclean microscope coverslip slides (VWR micro cover glass, 22 × 22 mm). Before imaging, each sample is given 15 min for the liposomes to settle. The fluorescence images were acquired in the "Galvano" mode in the Nikon user interface with a resolution typically set at 1024 × 1024 pixel.

Particle Size/Yield Analysis. Size of Janus liposomes was obtained by analyzing representative fluorescence images that typically contain several hundred liposomes per sample. To do so, the contour area of liposomes was first determined using "analyze particle" function in ImageJ (version: 1.54g); miscounted particles were subsequently inspected, and manually added or removed accordingly. The particle diameter ($2R$) was then derived from the area (πR^2) thus obtained. The Janus yield, which defines the fraction of Janus liposomes over all liposomes captured in fluorescence images, was manually determined.

RESULTS

Rationale for Lipid Selection. Two main strategies were taken in this work to achieve liquid−liquid phase separation (LLPS) in individual liposomes. Following the general organization framework of DOPC/DPPC/Chol, the first strategy examines alternative ternary lipid systems consisting of a low-melting lipid, a high-melting lipid and Chol, which similarly exploits the latter's role to liquefy the high-melting component and as a common solvent. The second approach attempts to make Chol-free Janus liposomes with binary lipid mixtures containing two low-melting lipids, with one containing short all-saturated acyl chains and the other unsaturated chain. Here, our working hypothesis is that the saturated (but short) lipids preferentially associate with like ones to produce the l_o domain through their favorable interchain van der Waals interactions and matching size. The structure, meting temperature (T_m) and bilayer thickness of the main lipids employed in this work are shown in Table 1. As detailed in the Experimental Section, liposomes containing these lipid mixtures are produced via gel-assisted hydration[8−10] at a temperature above T_m of all involved lipids. In our practice, we have found this a general method that constantly yields good quality liposome products and is also relatively insensitive to types of lipids employed.

Table 1. Main Lipids Investigated: Their Abbreviated Name, Phase-Transition Temperature (T_m), and Bilayer Thickness

l_o-forming lipids	l_d-forming lipids
1. DPPC (41°C[a]; 39.0 Å at 50°C[b]; Ref. 53)	2. DOPC (−17°C; 36.8 Å at 30°C; Ref. 54)
3. PSM (44.5°C; 38.9 Å at 45°C; Ref. 55)	4. DPhPC (< −120°C; 36.3 Å at 20°C; Ref. 53)
5. DMPC (24°C; 36.7 Å at 30°C; Ref. 53)	6. 16:1 PC (−36°C)
7. 13:0 PC (14°C)	8. 18:2 PC (−57°C)
9. 12:0 PC (−2°C; 33.0 Å at 20°C; Ref. 53)	10. 18:3 PC (−60°C)
11. 12:0 PG (−3°C; 29.9 Å at 20 °C; Ref. 56)	12. DOPG (−18°C; 36.3 Å at 20°C; Ref. 56)

[a]Phase transition temperature (T_m). [b]Bilayer thickness (temperature at which the thickness is measured).

In the remaining of this section, we first present results on screening for LLPS in ternary, cross-blended and binary lipid systems following liposome morphology determined by confocal fluorescence microscopy. For successful, high-yield products, their size distribution and yields are also provided. Mechanistic interpretations of such formations will be given separately in the following Discussion section.

Ternary Systems. As shown in Figure 2, Janus liposomes comprising DPPC/Chol together with either DPhPC or 16:1 PC as the low-melting component can be prepared in high yields of 87−94%. Similar to DOPC/DPPC/Chol liposomes produced by the same hydration method,[8] liposome sizes are broadly distributed from low to tens of μm, with the highest population appearing in the range of 5−20 μm. Interestingly, when DMPC is employed instead of DPPC as the high-melting lipid, Janus liposomes are obtained only when DPhPC serves as the low-melting partner (Figure 2c). Replacing DPhPC with either DOPC or 16:1 PC only gave products predominated by liposomes with no apparent global (Janus) phase separation (Figure S1). Subjecting these liposomes to additional temperature treatments, e.g., heating to 40, 45, or 50 °C followed by cooling at various rates, did not appreciably improve their Janus yields (data not shown). Zooming in further on individual liposomes, however, we could discern small, interspersed lipid domains across the entire liposome surface, as indicated by their periodic, regularly displaced green (l_o)/red (l_d) fluorescence intensity profiles (Figure S1). Thus, under conditions tested here, phase separation in these ternary liposomes does occur but fails to reach global scale.

While this investigation was motivated in part to generate stable Janus liposomes comprising mostly saturated lipids, we

https://doi.org/10.1021/acs.langmuir.5c01698
Langmuir 2025, 41, 19270−19281

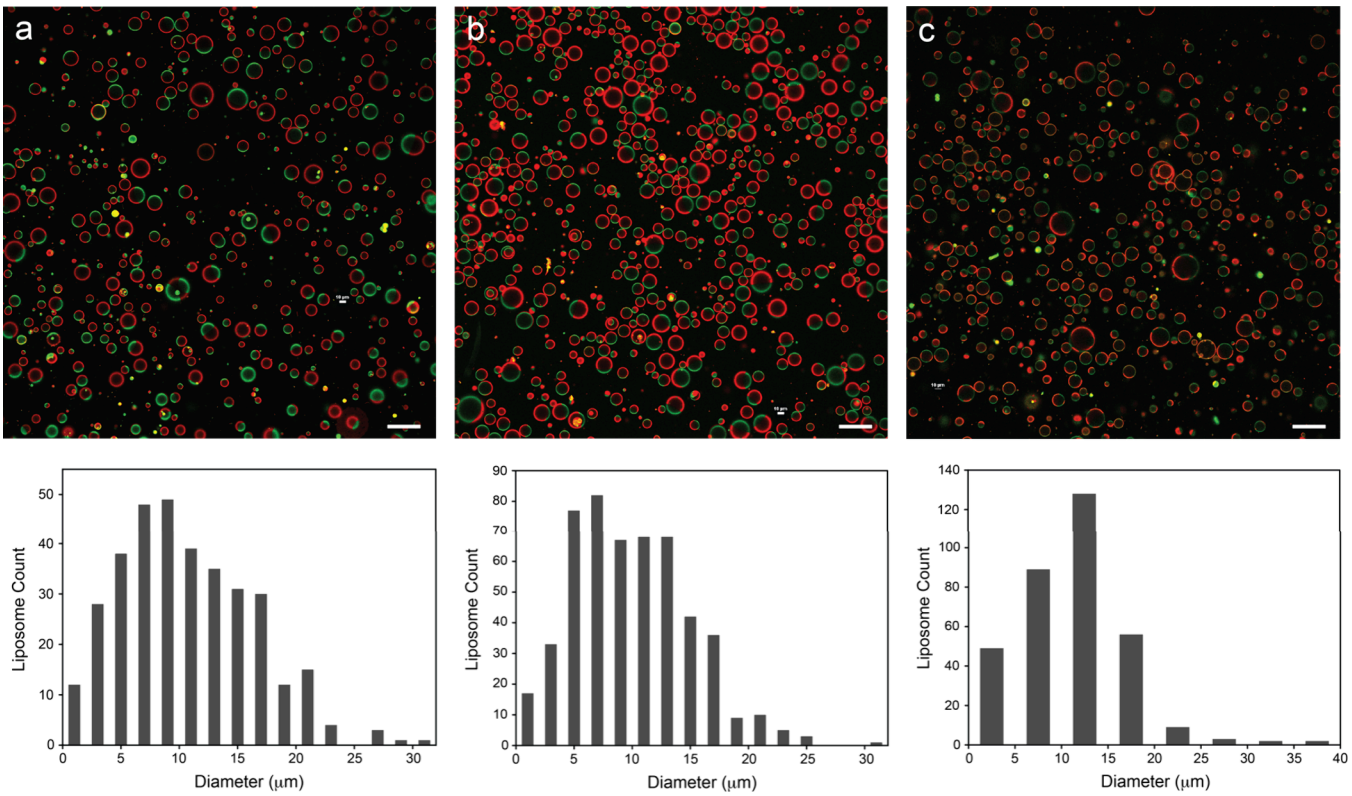

Figure 2. Fluorescence micrographs and size distribution of Janus liposomes featuring DPPC-/DMPC-containing ternary lipid combinations. (a) DPPC/DPhPC/Chol (35/35/30, mole ratio; Janus particle yield: 87%). (b) DPPC/16:1 PC/Chol (35/35/30; 94%). (c) DMPC/DPhPC/Chol (35/35/30; 61%). In each case, the corresponding size-distribution histogram is shown below the image. All liposomes in addition contain phase-indicating dyes, Bodipy-Chol (l_o) and rho-DOPC (l_d), at 0.1% each; 1 h hydration was conducted at 50 °C in (a) and (b) and 40 °C in (c). Scale bar: 50 μm.

included two polyunsaturated lipids, 18:2 and 18:3 PC, to establish the correlation, if any, between lipid unsaturation level and ease/yield of JL production. As shown in Figure 3a, DPPC/18:2 PC/Chol 35:35:30 mixtures produce JLs in decent yield (53%) upon hydration, which, however, are mixed with an appreciable fraction of liposomes with an oversized green (l_o) half. When 18:2 PC was replaced by 18:3 PC as the low-melting component, however, only single-phased l_o and l_d liposomes, presumably enriched with DPPC/Chol and 18:3 PC, respectively, were found (Figure 3b).

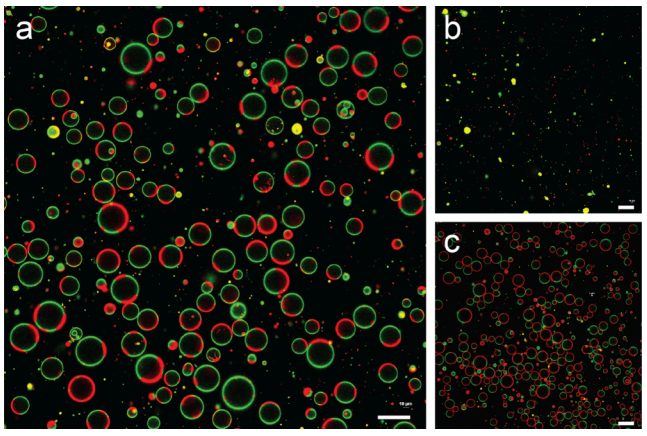

Figure 3. Fluorescence micrographs of liposomes prepared from polyunsaturated PC-containing ternary lipid combinations. (a) DPPC/18:2 PC/Chol (35/35/30) and (b) DPPC/18:3 PC/Chol (35/35/30), as compared with (c) DPPC/DOPC/Chol (35/35/30). All liposomes in addition contain phase-indicating dyes, Bodipy-Chol (l_o) and rho-DOPC (l_d), at 0.1% each; 1 h hydration at 50 °C was conducted in all cases. Scale bar: 50 μm.

Janus liposomes with PSM as the high-melting lipid were prepared in 70−80% yields when paired with DOPC, DPhPC and 16:1 PC (Figure 4). Compared to DPPC-based systems, these PSM JLs display several distinctive features. 1) Higher lipid hydration temperature. To prepare these liposomes in high yields, we found it necessary to run the hydration at 60 °C as opposed to 50 °C for DPPC. In the preparation with DOPC as the low-melting lipid, hydration at 50 or 55 °C suffered from low Janus yields and inconsistency, whereas with DPhPC, hydration at lower temperatures yielded mostly mixtures of single-phased particles (Figure S2). 2) More frequent formation of lipid clumps, an outcome likely due to expedited lipid hydration and vesiculation occurring at high temperature. 3) Lower liposome yields, both in particle and Janus production, when paired with 16:1 PC (Figure 4c).

Cross-Blended Systems. Besides new ternary JLs, previous section also reveals prevalent nonuniformity in lipid organization and physicochemical properties among differently configured l_o/l_d domains. For instance, PSM/Chol association is not to be taken as the same as that between DPPC and Chol, just as DMPC vs DPPC bilayers in their extent of hydration, despite that they are all broadly categorized as l_o domains. Prompted by such subtleties, we next examined if systems containing multiple low-/high-melting lipids would be sufficiently compatible to yield JLs. Besides answering our

https://doi.org/10.1021/acs.langmuir.5c01698
Langmuir 2025, 41, 19270−19281

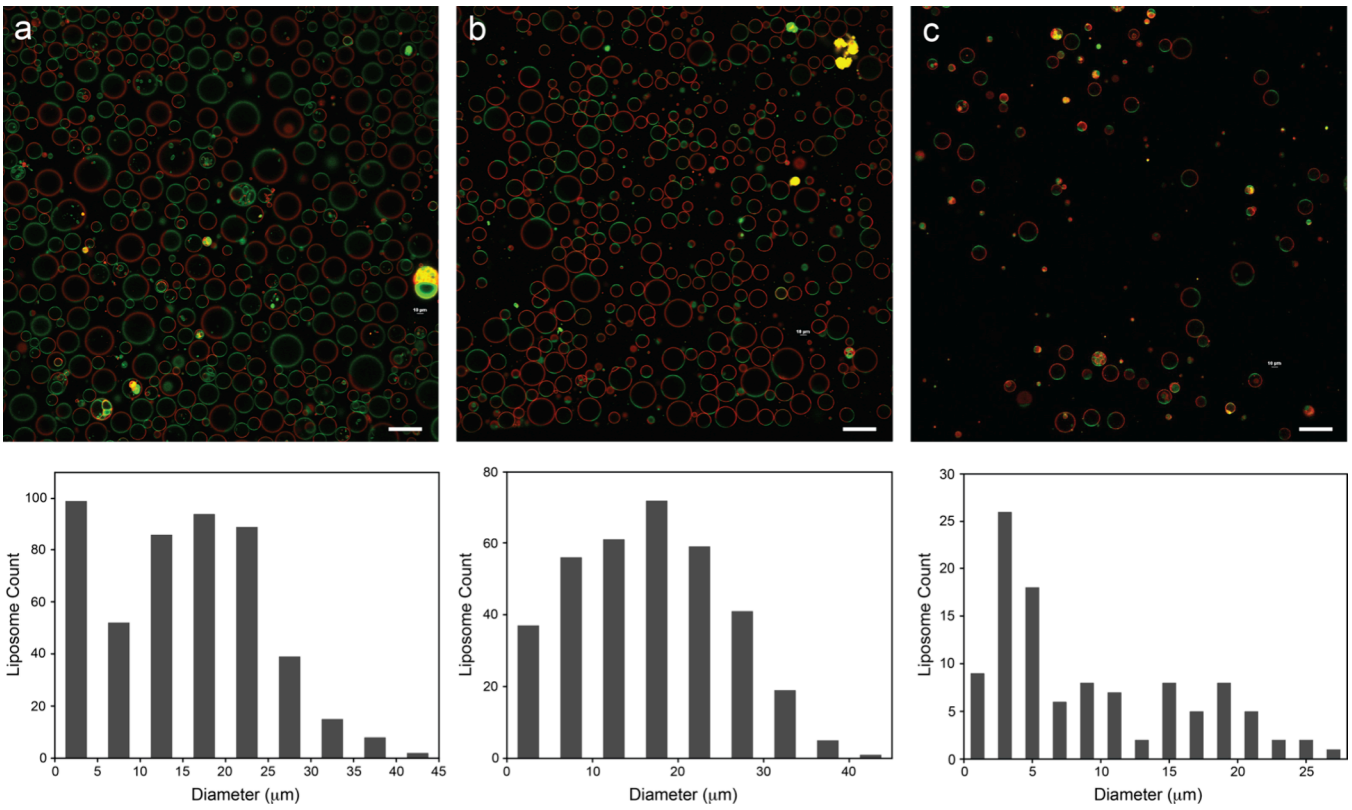

Figure 4. Fluorescence micrographs and size distribution of PSM-based ternary Janus liposomes. (a) PSM/DOPC/Chol (35/35/30, mole ratio; Janus particle yield: 79%); (b) PSM/DPhPC/Chol (35/35/30; 75%); (c) PSM/16:1 PC/Chol (35/35/30; 69%). All liposomes in addition contain phase-indicating dyes, Bodipy-Chol (l_o) and rho-DOPC (l_d), at 0.1% each; 1 h hydration at 60 °C was performed in all cases. Scale bar: 50 μm.

curiosity, this attempt may also yield new anisotropic, supermixed liposome models.

As shown in Figure 5, the quadruple system consisting of two high-melting lipids (DPPC and PSM) together with DPhPC and Chol produces JLs in 70% yield. Some liposomes appear oval instead of spherical shaped, likely due to osmotic imbalances inadvertently introduced during handling/transfer of small-volume liposome samples. When DPhPC was replaced by DOPC as the low-melting partner, however, JLs formed only sporadically and single-l_d-phased liposomes appeared instead as the predominant product (Figure S3). Similarly, 5-component JLs containing two high-melting lipids and two low-melting lipids together with Chol were also successfully made (Figure 5b). Here, however, the Janus yield was significantly lower (57%), as hydration at 60 °C produces a large fraction of single-l_d-phase, presumably DOPC-rich, liposomes.

Binary Systems. As shown in Figure 6, pairing DLPC (T_m: −2 °C) with a series of low-melting lipids yielded mostly single-phase and partially phase-separated liposomes. In the case of 1:1 mixed DLPC/DOPC, a minor but significant population of liposomes contains a single small green domain, presumably concentrated with all-saturated DLPC, whereas the majority of liposomes appeared to be single-phased (Figure 6a). Raising the fraction of DLPC from 50% to 75% did not appreciably enlarge the size of the green domain on individual liposomes, however (Figure S4). Assuming proportional uptake of both lipids in these liposomes, such insensitivity points to the inadequacy of Bodipy-Chol to properly reveal these new liquid phases. Likewise, no global phase separation was achieved when either 18:2 or 18:3 PC was used in place of DOPC (Figure S4). On the other hand, the pair of DLPC/DPhPC gave predominantly single-l_d-phased products mixed with a small fraction of liposomes containing similarly a single small l_o (green) domain (Figure 6b).

With the combination of DLPC/16:1PC, we again found single-l_d-phased liposomes to be the predominant product. Remarkably, Janus liposomes, with hallmarks of contrasted fluorescence between two hemispherical domains and neck formation around the phase boundary,[22,57] were also seen occasionally (Figure 6c). Despite its rare occurrence, such successful formation unambiguously demonstrates that *two dissimilar lipids can produce sufficient immiscibility to induce global LLPS—without the assistance by Chol*. Since these Janus liposomes display similar green fluorescence as those single-phased ones, moreover, we can rule out the possibility that Bodipy-Chol, the l_o fluorescent indicator spiked at 0.1 mol % in the sample, plays a significant role in their formation. This conclusion is further supported by another control measurement, in which ternary system of DLPC/16:1PC/Chol (35/35/30) was found to yield only single-l_d-phased liposomes (Figure S5). Assuming low kinetic barriers for lipid coalescence (such as the case of the JLs observed), we can further attribute the low JL yield to the lack of DLPC/16:1 PC coincorporation during lipid hydration. Indeed, there appears to be a small fraction of liposomes whose fluorescence matches the brighter side of the few JLs observed and exceeds that from most other single-phased liposomes (green arrows, Figure 6c).

Similarly, we have tested binary mixtures of C13:0 PC (T_m: 14 °C) pairing with a series of low-melting lipids. As shown in

https://doi.org/10.1021/acs.langmuir.5c01698
Langmuir 2025, 41, 19270−19281

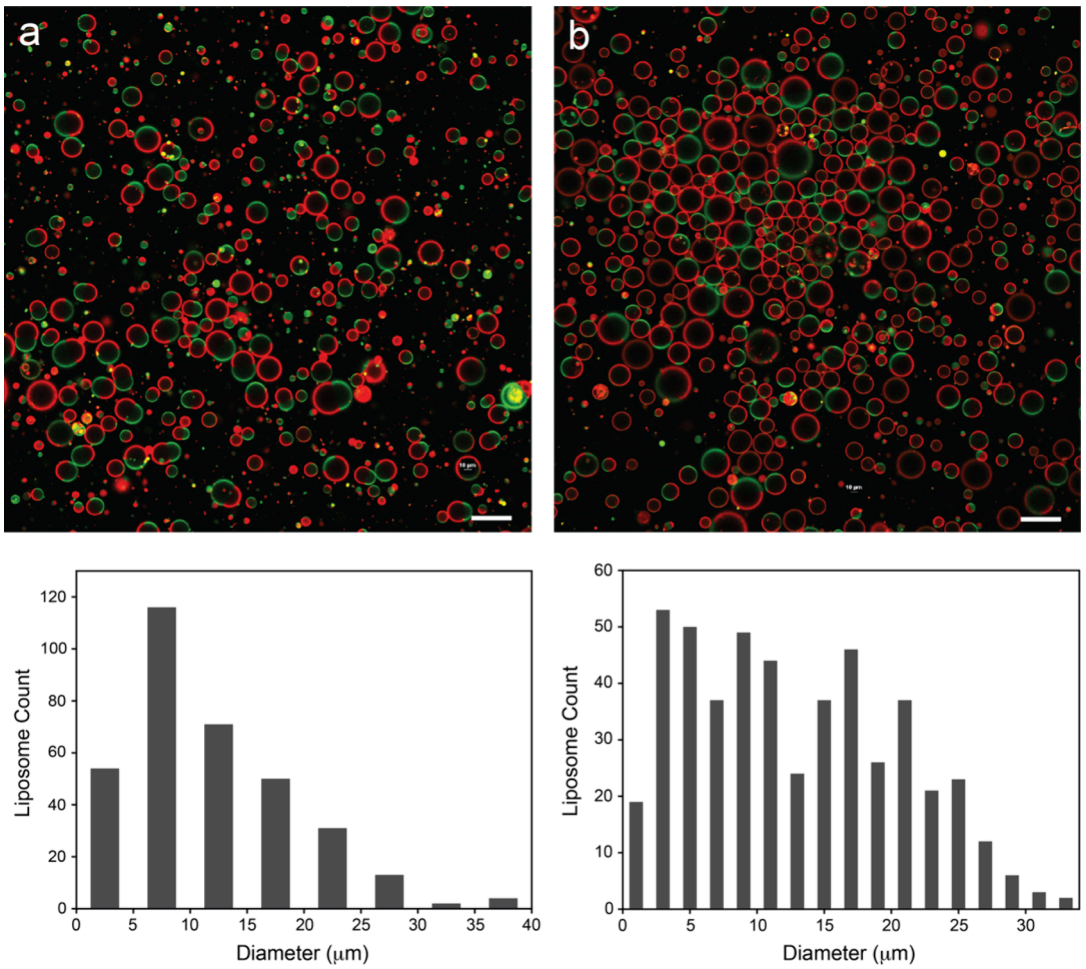

Figure 5. Fluorescence micrographs and size distribution of cross-blended Janus liposomes. (a) PSM/DPPC/DPhPC/Chol (15/20/35/30, mole ratio; Janus particle yield: 70%); (b) PSM/DPPC/DOPC/DPhPC/Chol (15/20/15/20/40; 57%). All liposomes in addition contain phase-indicating dyes, Bodipy-Chol (l_o) and rho-DOPC (l_d), at 0.1% each; 1 h hydration at 60 °C was performed in both cases. Scale bar: 50 μm.

Figure 7, 1:1 mixed C13:0 PC/DOPC gave single-l_d-phased liposomes as the sole product; similar results were obtained when DOPC was replaced by either DPhPC or 16:1 PC (Figure S6).

All lipid combinations that lead to global LLPS in individual liposomes and hence successful formation of JLs are summarized in Table 2.

Other Unsuccessful Cases. Besides the results presented above, a number of other binary lipid combinations were also tested and found unable to give JLs. A list of these unsuccessful cases, together with brief description of tested conditions and morphological appearance, is provided in the Supporting Information (Table S1).

■ DISCUSSION

Structural Features of Selected Lipids. Keeping Chol as the common solvent, we first examined ternary lipid combinations with PSM or DMPC serving as high-melting (l_o) lipids in place of DPPC, and DPhPC or 16:1 PC as low-melting (l_d) lipids replacing DOPC. Among these, PSM as a model sphingomyelin has been frequently employed in biomembrane studies related to lipid phase separation[58,59] and detergent-resistant membranes.[60] Structurally, the 3-OH and amide groups in sphingomyelin facilitate extensive intra/intermolecular hydrogen bonding not only among themselves but also with interfacial water molecules.[61,62] As a result, they typically display higher binding affinity toward Chol than do PC lipids (which normally can only act as H-bonding acceptor), yielding tight lipid bilayers with suppressed lipid rotation/diffusion.[63−65] DMPC[66,67] and 16:1 PC,[68] on the other hand, are often used alongside their homologues (DPPC and DOPC, respectively) in membrane characterization and liposome formulations. In contrast, DPhPC is unique in its archaeal origin characteristic of (tetramethyl) branched acyl chains that inhibit close interchain packing; this produces persistent disorder and slow dynamics in its bilayers − as manifested by its exceedingly broad melting temperature window spanning ±120 °C,[69] as well as high mechanical strength[70] and low membrane permeability.[71] While Janus liposomes based on DPhPC together with DPPC and Chol have been prepared by us previously,[10,72] liposome yields or its binary/ternary combinations with most other lipids included in this work have not.

DMPC vs DPPC vs PSM as L_o Lipids. The distinctive phase separation behaviors between DMPC- and DPPC-based ternary systems shown in Figure 2 may be understood as follows. First, considering hydrophobic mismatch in lipid acyl chains as a main driving force for phase separation,[73−75] the DMPC bilayer possesses a thickness comparable to that of DOPC (Table 1), which provides little hydrophobic surface

https://doi.org/10.1021/acs.langmuir.5c01698
Langmuir 2025, 41, 19270−19281

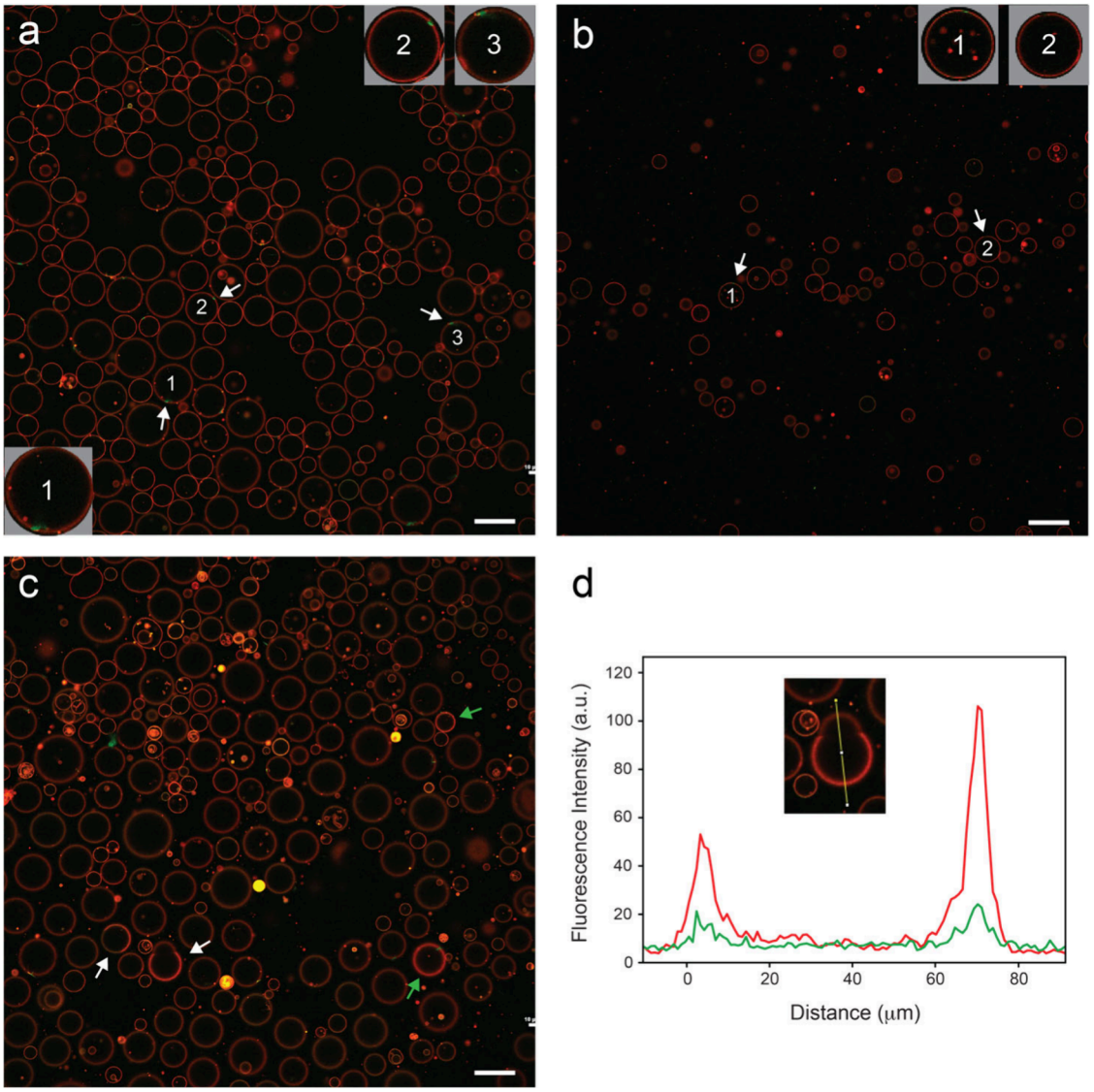

Figure 6. Fluorescence micrographs of binary liposomes. Lipid composition: (a) DLPC/DOPC (50/50); (b) DLPC/DPhPC (50/50); (c) DLPC/16:1 PC (50/50). All liposomes in addition contain phase-indicating dyes, Bodipy-Chol (l_o) and rho-DOPC (l_d), at 0.1% each; 1 h hydration at 50 °C was employed in all cases. In (a) and (b), the small green domain is marked out by white arrows on several liposomes (numbered and their zoomed-in images shown as insets). In (c), Janus liposomes (white arrow) and high-fluorescence liposomes (green arrow) are marked out accordingly. (d) Fluorescence intensity profile across a DLPC/16:1 PC Janus liposome (image shown as inset). Scale bar: 50 μm.

tension to promote large-scale segregation between the two. As a result, their phase separation features small kinetically trapped lipid domains unable to coalesce continuously. It should be noted that DMPC bilayers are expected to grow in thickness with the addition of Chol, e.g., from ∼40.1 Å (without Chol) to ∼44.1 Å (with 47% Chol) at 30 °C.[76] However, this remains to be too close to the thickness of DOPC/Chol bilayers, e.g., 46.2 Å (with 20% Chol) determined at 25 °C,[77] to mount a significant mismatch. By contrast, such a mismatch is accentuated by its l_o domain being ∼10 Å thicker than the corresponding l_d domain in the case of DPPC/DOPC/Chol.[28] Second, from the perspective of PC/Chol interactions, DPPC represents a stronger hydrogen-bonding partner to Chol and offers more shielded packing accommodation to the latter, than DMPC. As a result, DPPC lowers Chol's extent to hydrogen-bond with interfacial water molecules more substantially than DMPC, e.g., 0.4 water per Chol vs 1.1 water per Chol of DMPC, as revealed by molecular dynamics simulation.[36] Since interlipid H-bonding directly weakens the lipid hydration level at the lipid/water interface,[33,78,79] it follows that DMPC-based l_o domains are significantly more hydrated than DPPC's. Juxtaposed with l_d domains, which are still more hydrated,[33,34] these DMPC domains thus make up a less distinctive mismatch in H-bonding network and hydration, as compared to DPPC-based domains. This mismatch, in turn, creates different levels of surface tension[80] across dissimilar domains, driving their phase separation to a different degree. The two mechanisms discussed here are clearly correlated, in that the hydrophobic mismatch energy results largely from the entropic penalty of disrupting water H-bonding networks at the lipid/water interface.[75]

Janus liposomes with PSM as the high-melting lipid were prepared in 70−80% yields when paired with DOPC, DPhPC and 16:1 PC but at an elevated temperature relative to DPPC (Figure 4). More than covering their T_m difference, 3.5 °C

https://doi.org/10.1021/acs.langmuir.5c01698
Langmuir 2025, 41, 19270−19281

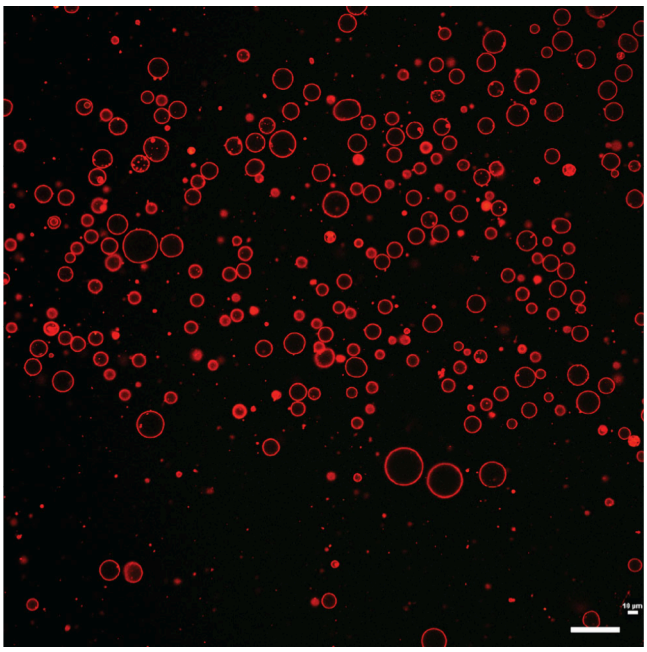

Figure 7. Fluorescence micrographs of 13:0 PC/DOPC binary liposomes upon 1 h hydration at 50 °C. Liposomes in addition contain phase-indicating dyes, Bodipy-Chol (l_o) and rho-DOPC (l_d), at 0.1% each. Scale bar: 50 μm.

(Table 1), this increase may reflect the extra thermal agitation needed to release PSM from its strong adhesion to the PVA gel layer. While its 3-OH and amide groups afford PSM extensive networking with neighboring lipids and water through intra- and intermolecular H-bonding, DPPC's H-bonding is more localized and less cohesive as it can function mostly only as a H-bonding acceptor.[62,81] PVA, on the other hand, is a well-known H-bonding polymer (through its hydroxyl pendants)—a feature frequently employed to modify its physical properties.[82,83]

Similar interaction/compatibility considerations also apply to the cross-blended systems (Figure 5). Specifically, the inability of PSM/DPPC/DOPC/Chol (15/20/35/30) to yield JLs may be attributed to 1) added incompatibilities due to copresence of DPPC and PSM and/or 2) elevated hydration temperature. Although seldomly investigated in comixtures, individual DPPC and PSM bilayers,[81,84−87] either alone or mixed with other components, have been frequently compared. For example, PSM is found to display lower diffusivity[84] and less melting cooperativity than DPPC in the presence of unsaturated lipids.[85] In the presence of Chol, moreover, PSM prefers to interact with the sterol's rough face, whereas DPPC prefers the smooth face.[86] Physicochemical distinctions as such compound the incompatibility between PSM and DPPC when mixed together, promoting their segregation and lowering their tendency to come off in the same liposome package during hydration.

DPhPC vs DOPC vs 16:1 PC as L_d Lipids. Several results above further reveal the superiority of DPhPC as the low-melting component in facilitating global lipid phase separation in Chol-containing lipid mixtures. Pairing with DMPC (e.g., Figure 2c), its bulky footprint—as shown by its large per-lipid occupancy area,[88] e.g., 80.5 Å^2 vs 72 Å^2 of DOPC, creates the needed mismatch in lipid packing that favors lateral lipid condensation/segregation, despite its similar bilayer thickness vis-à-vis DMPC (Table 1). Geometrically, its branched chains give rise to a relatively stout hydrocarbon base with respect to its PC headgroup, thus disfavoring close contact/packing with Chol, whose small headgroup (3β-OH) typically requires coverage/accommodation by neighboring PC lipids.[35,36] As observed by Engberg and co-workers,[89] it is the affinity of Chol to one and aversion to another that together determine the extent of phase separation in ternary systems. Since the packing incompatibility between DPhPC and Chol brings additional aversion into the system, it drives further the latter's association with saturated lipids and hence the phase separation. Structurally, DPhPC's tetramethyl side chains give rise to more extended perturbation and disorder when packed adjacent to straight-chain phospholipids; in comparison, DOPC's disorder originates mostly locally from its Δ9-*cis* double bonds. This important feature thus gives DPhPC an edge in assisting high-melting lipids to come off and remain associated in the same liposomes during hydration.

In comparison to DOPC and DPhPC, 16:1 PC as an l_d component has received less attention in lipid LLPS studies. Together with DPPC and Chol, it produces the highest JL yield of the present work (Figure 2b). By contrast, its JL yield when paired with PSM is significantly lower (Figure 4c), which may arise from its increasing rejection by PSM and Chol in the mixture. This is caused primarily by strong association between PSM and Chol (vs DPPC/Chol), with the added incompatibility between 16:1 PC and Chol being another potential contributor. Compared to DOPC, whose 18:1 chains match well with Chol's axial length when packed together in bilayers,[90] 16:1 PC's shortened acyl chains are expected to provide less accommodation to Chol, in particular, its aliphatic tail. Such incompatibility exists similarly in DPPC/16:1 PC/Chol, which, however, appears to be more than balanced out by less severe repulsion elsewhere in the system, i.e., weaker

Table 2. Lipid Combinations Capable of Producing Janus Liposomes (JLs)

Lipid combinations	Mixing ratios (mol %)	JL Yield (%)
DPPC/DPhPC/Chol	35/35/30	87
DPPC/16:1 PC/Chol	35/35/30	94
DMPC/DPhPC/Chol	35/35/30	61
DPPC/18:2 PC/Chol	35/35/30	53
PSM/DOPC/Chol	35/35/30	79
PSM/DPhPC/Chol	35/35/30	75
PSM/16:1 PC/Chol	35/35/30	69
PSM/DPPC/DPhPC/Chol	15/20/35/30	70
PSM/DPPC/DOPC/DPhPC/Chol	15/20/15/20/30	57
DLPC/16:1 PC	50/50	Extremely low; sporadic formation

https://doi.org/10.1021/acs.langmuir.5c01698
Langmuir 2025, 41, 19270−19281

association between DPPC and Chol (vs PSM/Chol) and weaker aversion of 16:1 PC toward DPPC (vs PSM). Such balanced interlipid interactions should allow a significant amount of 16:1 PC to exist in l_o domains[85] in DPPC/16:1 PC/Chol mixtures, increasing the overall cooperativity within the system and hence particle yields. Meanwhile, the higher hydration temperature used in making PSM/16:1 PC/Chol JLs may exacerbate Janus yield through promotion of uneven lipid liftoff during lipid hydration.

Impact of Unsaturation Level of L_d Lipids on JL Formation. Whereas successful JL formation confirms global phase separation in DPPC/18:2 PC/Chol ternary blend (Figure 3a), the presence of l_o-dominant liposomes in the products suggests disproportional lipid incorporation during lipid hydration/vesiculation—an outcome likely caused by increased incompatibility[91,92] between 18:2 PC and Chol due to their mismatched structural rigidity/flexibility. This trend is further verified by samples prepared from DPPC/18:3 PC/Chol 35:35:30 mixtures, which instead give nearly all single-phased l_o and l_d liposomes (Figure 3b). Taken together, these results stress the need to tailor the low-melting component to achieve global phase separation in ternary lipid systems: Since it takes Chol to assist the former's transfer into the l_o domain to establish as a minor component there, overly strong aversion between the two—as the case here due to polyunsaturation—depresses the needed transfer and hence dynamic lipid equilibration between the two phases.

Global LLPS in Binary Lipid Systems. The general flexibility in choosing l_d/l_o lipids, together with the difficulty of producing Chol-free JLs, established in last section once again underscores Chol's indispensable roles in facilitating and maintaining LLPS in lipid mixtures.[35−37,39,81] In a small amphiphilic package, Chol possesses not only sidedness (i.e., smooth/rough faces) with respect to its fused ring system but also heterogeneous rigidity/flexibility along its long axis. Such multifold structural asymmetry and heterogeneity, in turn, impart multivalency to its interaction with low- vs high-melting lipids, ordering one and liquefying the other while maintaining a dynamic liquid/liquid two-phase coexistence. Without Chol, therefore, complete LLPS in binary lipid systems will have to rely solely on managing the incompatibility and mismatch between the two components.

Three basic considerations are evaluated in this work accordingly. First, to bypass the need of having Chol to liquefy the high-melting lipid, saturated lipids with short acyl chains and low T_m are employed. As such, both lipids exist in liquid state at room temperature to start the separation. Second, to induce phase separation, the two lipids are chosen such that they bear significant hydrophobic mismatch when coassembled. Third, to further enhance their tendency of phase separation, lateral heterogeneities, such as H-bonding and charge pairing, are introduced into the binary mixtures through their headgroups.

Among ∼20 binary lipid combinations examined, only two prodglobal LLPS and JLs at very low yields DLPC/16:1 PC gives (Figure 6c) and DLPC/DOTAP (Table S1). With regard to suitable l_o lipid candidates in binary systems, the lipid length appears a more deciding factor than the headgroup identity. Compare DLPC (C12, Figure 6) with 13:0 PC (Figure 7), for example. Although the latter's stronger interlipid association (as indicated by its higher T_m) promotes higher segregation from the low-melting partners, its increased bilayer thickness lowers the hydrophobic mismatch between two liquid domains and hence their tendency to phase separate.

An important finding from LLPS in binary systems is that the resultant liquid phases differ significantly from Chol-induced l_d and l_o domains—as far as fluorescence evidence is concerned. Compared to ternary JLs, which display clear-cut red/green fluorescence split between l_d and l_o domains, both l_d and l_o phase-indicating dyes appeared to be enriched on the same side in DLPC/16:1 PC JLs (Figure 6d). Tentatively, we assign the domain with higher fluorescence intensity as the 16:1 PC-rich liquid phase and the less fluorescent side the DLPC-rich half. At the same time, it should be recognized that the absence of Chol in such phase separation would immediately disqualify Bodipy-Chol as a suitable indicator of these new liquid phases. To fully establish such formations, additional work is clearly needed, for example, by illuminating the lipid interactions and driving forces for phase separation. To achieve so, furthermore, a good starting point would be a reliable preparation method that enables such liposomes to be made in reasonable yields.

CONCLUSION

In this work, we have systematically examined >30 binary, ternary and cross-blended lipid systems as alternatives to DOPC/DPPC/Chol to yield global liquid−liquid phase separation (LLPS) within individual liposomes. Among these, eight ternary and cross-blended lipid combinations gave JLs in decent to high yields; while binary JLs were found to form only sporadically, they to our knowledge provide the very first demonstration of sterol-free, large-scale LLPS in free-floating lipid systems. In relation to the Chol-centered lipid raft model,[93−95] it is tempting to ponder whether binary LLPS could be at work in a similar fashion in Chol-absent native lipid settings,[96,97] e.g., bacterial/mitochondrial membranes. This work also reveals important nuances in fluid lipid organization that fall outside the general categorization of l_d/l_o lipid phases as the central rubric of lipid LLPS. To better understand binary phase segregation and its biophysical implications, further investigation, through e.g., spectroscopic characterization and computer simulation, is clearly needed. To use fluorescence spectroscopic and microscopic techniques in such efforts, in particular, having available new dye species specific to these lipid phases would be beneficial.

From the perspective of JLs as an anisotropic and soft colloidal material, this work in addition offers a number of new choices with improved chemical/mechanical stability and temperature window with respect to DOPC/DPPC/Chol. Together, these new lipid systems pave the way to diverse and wholistic future development of JLs as robust lipid models and colloidal building blocks.

ASSOCIATED CONTENT

Supporting Information

The Supporting Information is available free of charge at https://pubs.acs.org/doi/10.1021/acs.langmuir.5c01698.

Additional fluorescence images of liposomes prepared under conditions specified in the main text and a table listing all other binary lipid combinations tested (PDF)

https://doi.org/10.1021/acs.langmuir.5c01698
Langmuir 2025, 41, 19270−19281

AUTHOR INFORMATION

Corresponding Author

Wei Zhan − *Department of Chemistry and Biochemistry, Auburn University, Auburn, Alabama 36849, United States;* orcid.org/0000-0001-7096-9261; Email: wzz0001@auburn.edu

Author

Ayesha Akter − *Department of Chemistry and Biochemistry, Auburn University, Auburn, Alabama 36849, United States*

Complete contact information is available at: https://pubs.acs.org/10.1021/acs.langmuir.5c01698

Notes

The authors declare no competing financial interest.

ACKNOWLEDGMENTS

This work is supported by the National Science Foundation (Award CHE-2108243).

REFERENCES

(1) Perro, A.; Reculusa, S.; Ravaine, S.; Bourgeat-Lami, E.; Duguet, E. Design and Synthesis of Janus Micro- and Nanoparticles. *J. Mater. Chem.* **2005**, *15*, 3745−3760.

(2) Du, J.; O'Reilly, R. K. Anisotropic Particles with Patchy, Multicompartment and Janus Architectures: Preparation and Application. *Chem. Soc. Rev.* **2011**, *40*, 2402−2416.

(3) Walther, A.; Muller, A. H. E. Janus Particles: Synthesis, Self-Assembly, Physical Properties, and Applications. *Chem. Rev.* **2013**, *113*, 5194−5261.

(4) Kirillova, A.; Marschelke, C.; Synytska, A. Hybrid Janus Particles: Challenges and Opportunities for the Design of Active Functional Interfaces and Surfaces. *ACS Appl. Mater. Interface* **2019**, *11*, 9643−9671.

(5) Beales, P. A.; Vanderlick, T. K. Partitioning of Membrane-Anchored DNA between Coexisting Lipid Phases. *J. Phys. Chem. B* **2009**, *113*, 13678−13686.

(6) Beales, P. A.; Nam, J.; Vanderlick, T. K. Specific Adhesion between DNA-Functionalized "Janus" Vesicles: Size-Limited Clusters. *Soft Matter* **2011**, *7*, 1747−1755.

(7) Inaba, H.; Uemura, A.; Morishita, K.; Kohiki, T.; Shigenaga, A.; Otaka, A.; Matsuura, K. Light-Induced Propulsion of a Giant Liposome Driven by Peptide Nanofibre Growth. *Sci. Rep.* **2018**, *8*, 6243.

(8) Wang, M.; Liu, Z.; Zhan, W. Janus Liposomes: Gel-Assisted Formation and Bioaffinity-Directed Clustering. *Langmuir* **2018**, *34*, 7509−7518.

(9) Liu, Z.; Cui, J.; Zhan, W. Dipolar Janus Liposomes: Formation, Electrokinetic Motion and Self-Assembly. *Soft Matter* **2020**, *16*, 2177−2184.

(10) Liu, Z.; Cui, J.; Zhan, W. Rapid Access to Giant Unilamellar Liposomes with Upper Size Control: Membrane-Gated, Gel-Assisted Lipid Hydration. *Langmuir* **2020**, *36*, 13193−13200.

(11) Sharma, A.; Sharma, U. S. Liposomes in Drug Delivery: Progress and Limitations. *Int. J. Pharm.* **1997**, *154*, 123−140.

(12) Barenholz, Y. Doxil® - The First FDA-Approved Nano-Drug: Lessons Learned. *J. Controlled Release* **2012**, *160*, 117−134.

(13) Guimarães, D.; Cavaco-Paulo, A.; Nogueira, E. Design of Liposomes as Drug Delivery System for Therapeutic Applications. *Int. J. Pharm.* **2021**, *601*, 120571.

(14) Taylor, T. M.; Weiss, J.; Davidson, P. M.; Bruce, B. D. Liposomal Nanocapsules in Food Science and Agriculture. *Crit. Rev. Food Sci.* **2005**, *45*, 587−605.

(15) Nohynek, G. J.; Lademann, J.; Ribaud, C.; Roberts, M. S. *Grey Goo* on the Skin? Nanotechnology, Cosmetic and Sunscreen Safety. *Crit. Rev. Toxicol.* **2007**, *37*, 251−277.

(16) Zhang, J.; Grzybowski, B. A.; Granick, S. Janus Particle Synthesis, Assembly and Application. *Langmuir* **2017**, *33*, 6964−6977.

(17) Li, Z.; Fan, Q.; Yin, Y. Colloidal Self-Assembly Approaches to Smart Nanostructured Materials. *Chem. Rev.* **2022**, *122*, 4976−5067.

(18) Sánchez, S.; Soler, L.; Katuri, J. Chemically Powered Micro- and Nanomotors. *Angew. Chem., Int. Ed.* **2015**, *54*, 1414−1444.

(19) Fusi, A. D.; Li, Y.; Llopis-Lorente, A.; Patino, T.; van Hest, J. C. M.; Abdelmohsen, L. K. E. A. Achieving Control in Micro-/Nanomotor Mobility. *Angew. Chem., Int. Ed.* **2023**, *62*, No. e202214754.

(20) Zöttl, A.; Stark, H. Emergent Behavior in Active Colloids. *J. Phys.: Condes. Matter* **2016**, *28*, 253001.

(21) Bowick, M. J.; Fakhri, N.; Marchetti, M. C.; Ramaswamy, S. Symmetry, Thermodynamics, and Topology in Active Matter. *Phys. Rev. X* **2022**, *12*, 010501.

(22) Veatch, S. L.; Keller, S. L. Separation of Liquid Phases in Giant Vesicles of Ternary Mixtures of Phospholipids and Cholesterol. *Biophys. J.* **2003**, *85*, 3074−3083.

(23) Veatch, S. L.; Polozov, I. V.; Gawrisch, K.; Keller, S. L. Liquid Domains in Vesicles Investigated by NMR and Fluorescence Microscopy. *Biophys. J.* **2004**, *86*, 2910−2922.

(24) Davis, J. H.; Clair, J. J.; Juhasz, J. Phase Equilibria in DOPC/DPPC-d_{62}/Cholesterol Mixtures. *Biophys. J.* **2009**, *96*, 521−539.

(25) Veatch, S. L.; Soubias, O.; Keller, S. L.; Gawrisch, K. Critical Fluctuations in Domain-Forming Lipid Mixtures. *Proc. Natl. Acad. Sci. U.S.A.* **2007**, *104*, 17650−17655.

(26) Heberle, F. A.; Feigenson, G. W. Phase Separation in Lipid Membranes. *Cold Spring Harb. Perspect. Biol.* **2011**, *3*, a004630.

(27) Drolle, E.; Kucerka, N.; Hoopes, M. I.; Choi, Y.; Katsaras, J.; Karttunen, M.; Leonenko, Z. Effect of Melatonin and Cholesterol on the Structure of DOPC and DPPC Membranes. *Biochim. Biophys. Acta* **2013**, *1828*, 2247−2254.

(28) Heftberger, P.; Kollmitzer, B.; Rieder, A. A.; Amenitsch, H.; Pabst, G. In Situ Determination of Structure and Fluctuations of Coexisting Fluid Membrane Domains. *Biophys. J.* **2015**, *108*, 854−862.

(29) Kollmitzer, B.; Heftberger, P.; Podgornik, R.; Nagle, J. F.; Pabst, G. Bending Rigidities and Interdomain Forces in Membranes with Coexisting Lipid Domains. *Biophys. J.* **2015**, *108*, 2833−2842.

(30) Et-Thakafy, O.; Delorme, N.; Gaillard, C.; Mériadec, C.; Artzner, F.; Lopez, C.; Guyomarc'h, F. Mechanical Properties of Membranes Composed of Gel-Phase or Fluid-Phase Phospholipids Probed on Liposomes by Atomic Force Spectroscopy. *Langmuir* **2017**, *33*, 5117−5126.

(31) Lindblom, G.; Orädd, G.; Filippov, A. Lipid Lateral Diffusion in Bilayers with Phosphatidylcholine, Sphingomyelin and Cholesterol: An NMR Study of Dynamics and Lateral Phase Separation. *Chem. Phys. Lipids* **2006**, *141*, 179−184.

(32) Gu, R.-X.; Baoukina, S.; Tieleman, D. P. Phase Separation in Atomistic Simulations of Model Membranes. *J. Am. Chem. Soc.* **2020**, *142*, 2844−2856.

(33) M'Baye, G.; Mély, Y.; Duportail, G.; Klymchenko, A. S. Liquid Ordered and Gel Phases of Lipid Bilayers: Fluorescent Probes Reveal Close Fluidity but Different Hydration. *Biophys. J.* **2008**, *95*, 1217−1225.

(34) Kilin, V.; Glushonkov, O.; Herdly, L.; Klymchenko, A.; Richert, L.; Mely, Y. Fluorescence Lifetime Imaging of Membrane Lipid Order with a Ratiometric Fluorescent Probe. *Biophys. J.* **2015**, *108*, 2521−2531.

(35) Chiu, S. W.; Jakobsson, E.; Mashl, R. J.; Scott, H. L. Cholesterol-Induced Modifications in Lipid Bilayers: A Simulation Study. *Biophys. J.* **2002**, *83*, 1842−1853.

(36) Róg, T.; Pasenkiewicz-Gierula, M.; Vattulainen, I.; Karttunen, M. Ordering Effects of Cholesterol and Its Analogs. *Biochim. Biophys. Acta* **2009**, *1788*, 97−121.

(37) Róg, T.; Pasenkiewicz-Gierula, M.; Vattulainen, I.; Karttunen, M. What Happens if Cholesterol Is Made Smoother: Importance of Methyl Substituents in Cholesterol Ring Structure on Phosphatidylcholine-Sterol Interaction. *Biophys. J.* **2007**, *92*, 3346−3357.

(38) Mills, T. T.; Toombes, G. E. S.; Tristram-Nagle, S.; Smilgies, D.-M.; Feigenson, G. W.; Nagle, J. F. Order Parameters and Areas in Fluid-Phase Oriented Lipid Membrane Using Wide Angle X-Ray Scattering. *Biophys. J.* **2008**, *95*, 669−681.
(39) Wilson, K. J.; Nguyen, H. Q.; Gervay-Hague, J.; Keller, S. L. Sterol-Lipids Enable Large-Scale, Liquid-Liquid Phase Separation in Bilayer Membranes of Only Two Components. *Proc. Natl. Acad. Sci. U.S.A.* **2024**, *121*, No. e2401241121.
(40) Marsh, D. Cholesterol-Induced Fluid Membrane Domains: A Compendium of Lipid-Raft Ternary Phase Diagrams. *Biochim. Biophys. Acta* **2009**, *1788*, 2114−2123.
(41) Klein, R. A. The Detection of Oxidation in Liposome Preparations. *Biochim. Biophys. Acta* **1970**, *210*, 486−489.
(42) Sankhagowit, S.; Wu, S.-H.; Biswas, R.; Riche, C. T.; Povinelli, M. L.; Malmstadt, N. The Dynamics of Giant Unilamellar Vesicle Oxidation Probed by Morphological Transitions. *Biochim. Biophys. Acta* **2014**, *1838*, 2615−2624.
(43) Fidorra, M.; Garcia, A.; Ipsen, J. H.; Härtel, S.; Bagatolli, L. A. Lipid Domains in Giant Unilamellar Vesicles and Their Correspondence with Equilibrium Thermodynamic Phases: A Quantitative Fluorescence Microscopy Imaging Approach. *Biochim. Biophys. Acta* **2009**, *1788*, 2142−2149.
(44) Chiang, Y.-W.; Shimoyama, Y.; Feigenson, G. W.; Freed, J. H. Dynamic Molecular Structure of DPPC-DLPC-Cholesterol Ternary Lipid System by Spin-Label Electron Spin Resonance. *Biophys. J.* **2004**, *87*, 2483−2496.
(45) Veatch, S. L.; Gawrisch, K.; Keller, S. L. Closed-Loop Miscibility Gap and Quantitative Tie-Lines in Ternary Membranes Containing Diphytanoyl PC. *Biophys. J.* **2006**, *90*, 4428−4436.
(46) Garidel, P.; Johann, C.; Blume, A. Thermodynamics of Lipid Organization and Domain Formation in Phospholipid Bilayers. *J. Liposome Res.* **2000**, *10*, 131−158.
(47) Lohner, K.; Latal, A.; Degovics, G.; Garidel, P. Packing Characteristics of A Model System Mimicking Cytoplasmic Bacterial Membranes. *Chem. Phys. Lipids* **2001**, *111*, 177−192.
(48) Kato, A.; Tsuji, A.; Yanagisawa, M.; Saeki, D.; Juni, K.; Morimoto, Y.; Yoshikawa, K. Phase Separation on a Phospholipid Membrane Inducing a Characteristic Localization of DNA Accompanied by Its Structural Transition. *J. Phys. Chem. Lett.* **2010**, *1*, 3391−3395.
(49) Papahadjopoulos, D.; Vail, W. J.; Newton, C.; Nir, S.; Jacobson, K.; Poste, G.; Lazo, R. Studies on Membrane Fusion. III. The Role of Calcium-Induced Phase Changes. *Biochim. Biophys. Acta* **1977**, *465*, 579−598.
(50) Silvius, J. R.; Gagné, J. Calcium-Induced Fusion and Lateral Phase Separations in Phosphatidylcholine-Phosphatidylserine Vesicles. Correlation by Calorimetric and Fusion Measurements. *Biochemistry* **1984**, *23*, 3241−3247.
(51) Korlach, J.; Schwille, P.; Webb, W. W.; Feigenson, G. W. Characterization of Lipid Bilayer Phases by Confocal Microscopy and Fluorescence Correlation Spectroscopy. *Proc. Natl. Acad. Sci. U.S.A.* **1999**, *96*, 8461−8466.
(52) Frolov, V. A. J.; Chizmadzhev, Y. A.; Cohen, F. S.; Zimmerberg, J. "Entropic Traps" in the Kinetics of Phase Separation in Multicomponent Membranes Stabilize Nanodomains. *Biophys. J.* **2006**, *91*, 189−205.
(53) Kucerka, N.; Nieh, M.-P.; Katsaras, J. Fluid Phase Lipid Areas and Bilayer Thicknesses of Commonly Used Phosphatidylcholines as a Function of Temperature. *Biochim. Biophys. Acta* **2011**, *1808*, 2761−2771.
(54) Pan, J.; Tristram-Nagle, S.; Nagle, J. F. Effect of Cholesterol on Structural and Mechanical Properties of Membranes Depends on Lipid Chain Saturation. *Phys. Rev. E* **2009**, *80*, 021931.
(55) Doktorova, M.; Kucerka, N.; Kinnun, J. J.; Pan, J.; Marquardt, D.; Scott, H. L.; Venable, R. M.; Pastor, R. W.; Wassall, S. R.; Katsaras, J.; Heberle, F. A. Molecular Structure of Sphingomyelin in Fluid Phase Bilayers Determined by the Joint Analysis of Small-Angle Neutron and X-ray Scattering Data. *J. Phys. Chem. B* **2020**, *124*, 5186−5200.
(56) Pan, J.; Heberle, F. A.; Tristram-Nagle, S.; Szymanski, M.; Koepfinger, M.; Katsaras, J.; Kucerka, N. Molecular Structures of Fluid Phase Phosphatidylglycerol Bilayers as Determined by Small Angle Neutron and X-Ray Scattering. *Biochim. Biophys. Acta* **2012**, *1818*, 2135−2148.
(57) Baumgart, T.; Hess, S. T.; Webb, W. W. Imaging Coexisting Fluid Domains in Biomembrane Models Coupling Curvature and Line Tension. *Nature* **2003**, *425*, 821−824.
(58) Veatch, S. L.; Keller, S. L. Miscibility Phase Diagrams of Giant Vesicles Containing Sphingomyelin. *Phys. Rev. Lett.* **2005**, *94*, 148101.
(59) Caritá, A. C.; Mattei, B.; Domingues, C. C.; de Paula, E.; Riske, K. A. Effect of Triton X-100 on Raft-Like Lipid Mixtures: Phase Separation and Selective Solubilization. *Langmuir* **2017**, *33*, 7312−7321.
(60) Heerklotz, H. Triton Promotes Domain Formation in Lipid Raft Mixtures. *Biophys. J.* **2002**, *83*, 2693−2701.
(61) Quinn, P. J.; Wolf, C. The Liquid-Ordered Phase in Membranes. *Biochim. Biophys. Acta* **2009**, *1788*, 33−46.
(62) Slotte, J. P. The Importance of Hydrogen Bonding in Sphingomyelin's Membrane Interactions with Co-Lipids. *Biochim. Biophys. Acta* **2016**, *1858*, 304−310.
(63) Halling, K. K.; Ramstedt, B.; Nyström, J. H.; Slotte, J. P.; Nyholm, T. K. M. Cholesterol Interactions with Fluid-Phase Phospholipids: Effect on the Lateral Organization of the Bilayer. *Biophys. J.* **2008**, *95*, 3861−3871.
(64) Jaikishan, S.; Slotte, J. P. Effect of Hydrophobic Mismatch and Interdigitation on Sterol/Sphingomyelin Interaction in Ternary Bilayer Membranes. *Biochim. Biophys. Acta* **2011**, *1808*, 1940−1945.
(65) Petruzielo, R. S.; Heberle, F. A.; Drazba, P.; Katsaras, J.; Feigenson, G. W. Phase Behavior and Domain Size in Sphingomyelin-Containing Lipid Bilayers. *Biochim. Biophys. Acta* **2013**, *1828*, 1302−1313.
(66) Makino, K.; Yamada, T.; Kimura, M.; Oka, T.; Ohshima, H.; Kondo, T. Temperature- and Ionic Strength-Induced Conformational Changes in the Lipid Head Group Region of Liposomes as Suggested by Zeta Potential Data. *Biophys. Chem.* **1991**, *41*, 175−183.
(67) Anderson, M.; Omri, A. The Effect of Different Lipid Components on the In Vitro Stability and Release Kinetics of Liposome Formulations. *Drug Delivery* **2004**, *11*, 33−39.
(68) Feigenson, G. W. Partitioning of a Fluorescent Phospholipid Between Fluid Bilayers: Dependence on Host Lipid Acyl Chains. *Biophys. J.* **1997**, *73*, 3112−3121.
(69) Lindsey, H.; Petersen, N. O.; Chan, S. I. Physicochemical Characterization of 1,2-Diphytanoyl-*sn*-Glycero-3-Phosphocholine in Model Membrane Systems. *Biochim. Biophys. Acta* **1979**, *555*, 147−167.
(70) Shinoda, W.; Mikami, M.; Baba, T.; Hato, M. Molecular Dynamics Study on the Effect of Chain Branching on the Physical Properties of Lipid Bilayers: Structural Stability. *J. Phys. Chem. B* **2003**, *107*, 14030−14035.
(71) Shinoda, W.; Mikami, M.; Baba, T.; Hato, M. Molecular Dynamics Study on the Effects of Chain Branching on the Physical Properties of Lipid Bilayers: 2. Permeability. *J. Phys. Chem. B* **2004**, *108*, 9346−9356.
(72) Cui, J.; Jin, H.; Zhan, W. Enzyme-Free Active Liposome Motion via Asymmetrical Lipid Efflux. *Langmuir* **2022**, *38*, 11468−11477.
(73) Lehtonen, J. Y. A.; Holopainen, J. M.; Kinnunen, P. K. J. Evidence for the Formation of Microdomains in Liquid Crystalline Large Unilamellar Vesicles Caused by Hydrophobic Mismatch of the Constituent Phospholipids. *Biophys. J.* **1996**, *70*, 1753−1760.
(74) Kuzmin, P. I.; Akimov, S. A.; Chizmadzhev, Y. A.; Zimmerberg, J.; Cohen, F. S. Line Tension and Interaction Energies of Membrane Rafts Calculated from Lipid Splay and Tilt. *Biophys. J.* **2005**, *88*, 1120−1133.
(75) Wallace, E. J.; Hooper, N. M.; Olmsted, P. D. Effect of Hydrophobic Mismatch on Phase Behavior of Lipid Membranes. *Biophys. J.* **2006**, *90*, 4104−4118.

https://doi.org/10.1021/acs.langmuir.5c01698
Langmuir 2025, 41, 19270−19281

(76) Pencer, J.; Nieh, M.-P.; Harroun, T. A.; Krueger, S.; Adams, C.; Katsaras, J. Bilayer Thickness and Thermal Response of Dimyristoylphosphatidylcholine Unilamellar Vesicles Containing Cholesterol, Ergosterol and Lanosterol: A Small-Angle Neutron Scattering Study. *Biochim. Biophys. Acta* **2005**, *1720*, 84−91.
(77) Gallová, J.; Uhríková, D.; Islamov, A.; Kuklin, A.; Balgavý, P. Effect of Cholesterol on the Bilayer Thickness in Unilamellar Extruded DLPC and DOPC Liposomes: SANS Contrast Variation Study. *Gen. Physiol. Biophys.* **2004**, *23*, 113−128.
(78) Boggs, J. M. Lipid Intermolecular Hydrogen Bonding: Influence on Structural Organization and Membrane Function. *Biochim. Biophys. Acta* **1987**, *906*, 353−404.
(79) Chiu, S. W.; Vasudevan, S.; Jakobsson, E.; Mashl, R. J.; Scott, H. L. Structure of Sphingomyelin Bilayers: A Simulation Study. *Biophys. J.* **2003**, *85*, 3624−3635.
(80) Alarcón, L. M.; de los Angeles Frías, M.; Morini, M. A.; Sierra, M. B.; Appignanesi, G. A.; Disalvo, E. A. Water Populations in Restricted Environments of Lipid Membrane Interphases. *Eur. Phys. J. E* **2016**, *39*, 94.
(81) Niemelä, P.; Hyvönen, M. T.; Vattulainen, I. Structure and Dynamics of Sphingomyelin Bilayer: Insight Gained through Systematic Comparison to Phosphatidylcholine. *Biophys. J.* **2004**, *87*, 2976−2989.
(82) Hodge, R. M.; Bastow, T. J.; Edward, G. H.; Simon, G. P.; Hill, A. J. Free Volume and the Mechanism of Plasticization in Water-Swollen Poly(vinyl alcohol). *Macromolecules* **1996**, *29*, 8137−8143.
(83) Shi, S.; Peng, X.; Liu, T.; Chen, Y.-N.; He, C.; Wang, H. Facile Preparation of Hydrogen-Bonded Supramolecular Polyvinyl Alcohol-Glycerol Gels with Excellent Thermoplasticity and Mechanical Properties. *Polymer* **2017**, *111*, 168−176.
(84) Filippov, A. V.; Rudakova, M. A.; Munavirov, B. V. Lateral Diffusion in Sphingomyelin Bilayers. *Magn. Reson. Chem.* **2010**, *48*, 945−950.
(85) Kullberg, A.; Ekholm, O. O.; Slotte, J. P. Miscibility of Sphingomyelins and Phosphatidylcholines in Unsaturated Phosphatidylcholine Bilayers. *Biophys. J.* **2015**, *109*, 1907−1916.
(86) Sodt, A. J.; Pastor, R. W.; Lyman, E. Hexagonal Substructure and Hydrogen Bonding in Liquid-Ordered Phases Containing Palmitoyl Sphingomyelin. *Biophys. J.* **2015**, *109*, 948−955.
(87) van Duyl, B. Y.; Ganchev, D.; Chupin, V.; de Kruijff, B.; Killian, J. A. Sphingomyelin Is Much More Effective Than Saturated Phosphatidylcholine in Excluding Unsaturated Phosphatidylcholine from Domains Formed with Cholesterol. *FEBS Lett.* **2003**, *547*, 101−106.
(88) Tristram-Nagle, S.; Kim, D. J.; Akhunzada, N.; Kucerka, N.; Mathai, J. C.; Katsaras, J.; Zeidel, M.; Nagle, J. F. Structure and Water Permeability of Fully Hydrated DiphytanoylPC. *Chem. Phys. Lipids* **2010**, *163*, 630−637.
(89) Engberg, O.; Hautala, V.; Yasuda, T.; Dehio, H.; Murata, M.; Slotte, J. P.; Nyholm, T. K. M. The Affinity of Cholesterol for Different Phospholipids Affects Lateral Segregation in Bilayers. *Biophys. J.* **2016**, *111*, 546−556.
(90) Róg, T.; Martinez-Seara, H.; Pasenkiewicz-Gierula, M.; Vattulainen, I.; Karttunen, M.; Reigada, R. Interplay of Unsaturated Phospholipids and Cholesterol in Membranes: Effect of the Double-Bond Position. *Biophys. J.* **2008**, *95*, 3295−3305.
(91) Niu, S.-L.; Litman, B. J. Determination of Membrane Cholesterol Partition Coefficient Using a Lipid Vesicle-Cyclodextrin Binary System: Effect of Phospholipid Acyl Chain Unsaturation and Headgroup Composition. *Biophys. J.* **2002**, *83*, 3408−3415.
(92) Kucerka, N.; Marquardt, D.; Harroun, T. A.; Nieh, M.-P.; Wassall, S. R.; de Jong, D. H.; Schäfer, L. V.; Marrink, S. J.; Katsaras, J. Cholesterol in Bilayers with PUFA Chains: Doping with DMPC or POPC Results in Sterol Reorientation and Membrane-Domain Formation. *Biochemistry* **2010**, *49*, 7485−7493.
(93) Brown, D. A.; London, E. Functions of Lipid Rafts in Biological Membranes. *Annu. Rev. Cell Dev. Biol.* **1998**, *14*, 111−136.
(94) Simons, K.; Vaz, W. L. C. Model Systems, Lipid Rafts, and Cell Membranes. *Annu. Rev. Biophys. Biomol. Struct.* **2004**, *33*, 269−295.
(95) Simons, K.; Sampaio, J. L. Membrane Organization and Lipid Rafts. *Cold Spring Harb. Perspect. Biol.* **2011**, *3*, a004697.
(96) Jain, M. K. *Introduction to Biological Membranes*, 2nd ed.; John Wiley & Sons, Inc.: New York, 1988.
(97) Mouritsen, O. G.; Zuckermann, M. J. What's So Special About Cholesterol? *Lipids* **2004**, *39*, 1101−1113.

https://doi.org/10.1021/acs.langmuir.5c01698
Langmuir 2025, 41, 19270−19281